Molecular Vision 2017; 23:160-170 <http://www.molvis.org/molvis/v23/160>
Received 24 January 2017 | Accepted 22 March 2017 | Published 24 March 2017

© 2017 Molecular Vision

Knock-in of Cx46 partially rescues fiber defects in lenses lacking Cx50

Eddie Wang, Andrew Geng, Richard Seo, Ankur Maniar, Xiaohua Gong

(The first two authors contributed equally to this work.)

School of Optometry and Vision Science Program, University of California, Berkeley, Berkeley, CA

Purpose: Connexins 46 (Cx46) and 50 (Cx50) support lens development and homeostasis. Knockout (KO) of Cx50, but not Cx46, causes defects in lens fiber organization, F-actin enrichment, gap junction (GJ) size, ball-and-socket (BS) maturation, and GJ-associated protein distributions. To further determine the unique roles of Cx50 and Cx46, we investigated whether these defects persisted in Cx46 knock-in (Ki) lenses. Ki mice had Cx46 knocked-in to their Cx50 loci, where it was expressed under endogenous Cx50 promoters.
Methods: Fiber cell morphology and the distribution of lens membrane/cytoskeleton proteins from wild-type (WT), Ki, and Cx50 KO mice were visualized by immunofluorescent labeling and confocal microscopy.
Results: Cx46 Ki partially rescued Cx50 KO lens fiber defects. Three-week-old Ki lens fibers had typical F-actin distributions but were nonuniformly sized and disorganized. The Cx-associated proteins zonula occludens-1 (ZO-1) and β-dystroglycan (βDys) no longer localized to the nuclei but remained absent from GJs. BS formed, but this occurred with lower than WT frequency. BS appeared with greater frequency in 8-week-old Ki lenses, but so did aberrant balloon-like structures similar to those in Cx50 KO lenses. Unexpectedly, 8-week-old Cx50 KO and Ki cortical lens fibers were no longer disorganized.
Conclusions: Cx identity is important for some aspects of fiber development (organization, Cx association with ZO-1 and βDys) but not others (F-actin enrichment). Either Cx supports BS maturation, but the sparsity of BS and presence of balloon-like structures in Ki lenses suggest that Cx50 is more capable of doing so. The partial rescue of BS structures may support the rapid growth of cortical fibers to the improved growth of Ki lenses compared to Cx50 KO lenses at young ages. Neither absence of Cx50 nor presence of Ki Cx46 affects cortical fiber cell organization by the age of 8 weeks.

Gap junctions (GJs) are clusters of dynamic membrane channels that allow for intercellular transport of small molecules and inorganic ions. GJ channels connect neighboring cells via head-to-head docking of transmembrane hemichannels, where each hemichannel is itself assembled from six connexin (Cx) protein subunits. The Cx protein family comprises about 20 members, with one or more isoforms being used to assemble each channel. Different isoform combinations result in channels with varying permeability, electrophysiology, and ability to be regulated [1-3]. Genetic manipulation of Cx has allowed for the dissection of individual isoform properties and the discovery of channel-dependent and independent functions in diverse tissues, including the ocular lens [2,4-7].

The lens is an avascular, nearly solid mass of cells that is reliant on extensive GJ-mediated coupling. An epithelial monolayer lines the surface of the anterior hemisphere, while the bulk mass is composed of highly elongated fiber cells. Throughout life, new fibers form as epithelial cells near the lens equator undergo differentiation, displacing older ones in from the lens surface. Lens fibers interdigitate with their neighbors by forming ball-and-socket (BS) structures and protrusions. BSs are GJ-enriched regions where the membrane of one fiber cell appears to bulge into a neighboring fiber cell [8,9]. Protrusions are actin-enriched structures that emanate from fiber vertices and lack GJs [9]. Lens fibers eventually lose their nuclei and other intracellular organelles as they undergo further maturation [10,11]. As a result, only the epithelial cells and peripheral fibers are metabolically active. GJs are critical to this arrangement, as they allow the active cells at the cortex to maintain homeostasis in the mature fibers.

Three types of Cx are expressed in the lens, namely Cx43, Cx46, and Cx50, which are encoded by the *Gja1*, *Gja3*, and *Gja8* genes, respectively. Cx43 is expressed only in the epithelial cells while Cx46 is first expressed when epithelial cells differentiate into fibers. Cx50 is highly expressed in both epithelial cells and fibers [2]. Past studies have focused on determining the isoform-specific roles of Cx46 and Cx50 in lens development and homeostasis. *Gja3*$^{-/-}$ knockout (KO) mice lacking Cx46 develop normal size lenses, with nuclear

Correspondence to: Xiaohua Gong, 693 Minor Hall, University of California, Berkeley, Berkeley, CA 94720, Phone: (510) 642-2491 FAX: (510) 642-5086; email: xgong@berkeley.edu

cataracts attributed to aberrant proteolysis [12]. *Gja8*$^{-/-}$ KO mice lacking Cx50 develop significantly smaller lenses with mild, pulverulent cataracts [13,14]. This growth defect is attributed to reduced early postnatal proliferation of lens epithelial cells [15]. In addition, only Cx50 was found to respond to mitogen-activated protein kinase (MAPK) and phosphoinositide 3-kinase (PI3K) pathway signaling and to promote channel-independent differentiation, while only Cx46 was found to transport glutathione to the lens core [16-20]. These and other studies suggest that Cx50 is critical to lens growth and differentiation, whereas Cx46 is more critical to lens transparency.

Knock-in (Ki) mice have their Cx50 loci homozygously replaced with Cx46 (*Gja3*$^{+/+}$ *Gja8(α3/α3)*) [21]. These mice provide a model for determining unique and redundant functions between Cx50 and Cx46 in lens fibers. Ki lenses are clear and between wild-type (WT) and Cx50 KO lenses in size. Additional studies have found that Ki lenses have recovered resting voltages, partially improved coupling conductance in differentiating fibers, and slightly improved postnatal epithelial cell proliferation rates, demonstrating the partial ability of Cx46 to substitute for Cx50 [22,23]. Therefore, we sought to examine whether certain Cx50 KO fiber cell defects that we had observed previously were also restored in Ki lenses. These defects included regions of disorganized fibers, atypical F-actin distributions, mistrafficking of Cx-associated proteins, small-sized GJ plaques, and lack of mature BSs [24]. Our results show that many but not all Cx50 KO phenotypes were rescued, which may partially explain the beneficial effects of knocking-in Cx46.

METHODS

Animals: Mouse care and breeding were performed according to the Animal Care and Use Committee (ACUC)-approved animal protocol (University of California Berkeley) and the Association for Research in Vision and Ophthalmology (ARVO) Statement for the Use of Animals in Ophthalmic and Vision Research. *Gja8*$^{-/-}$ mice and Ki mice expressing four alleles of Cx46 were described previously and maintained in the C57BL6/J background [14,21]. The C57BL6/J strain was also used for WT mice.

Immunohistochemistry: Mouse eyes were collected immediately after euthanasia by CO_2 inhalation. Lenses were dissected into PBS (137 mM NaCl, 2.7 mM KCl, 10 mM Na_2HPO_4, 1.8 mM KH_2PO_4, pH 7.4) and then immersed into 4% paraformaldehyde (PFA; Electron Microscopy Sciences, Hatfield, PA) in PBS at 37 °C for 30 min. After fixation, lenses were washed 3X with PBS and cut into 150-µm-thick sections with a vibratome (Leica VT1000 S; Leica, Wetlar, Germany). Sections were then postfixed with 4% PFA in PBS for 2 min at room temperature and washed 3X with PBS before staining.

All sections were permeabilized and blocked in PBS (3% w/v bovine serum albumin [BSA; Research Products International, Prospect, IL], 3% v/v normal goat serum (Vector Laboratories, Burlingame, CA), 0.3% v/v Triton X-100 [Sigma-Aldrich, St. Louis, MO] in PBS) for 1 h. For antibody labeling, sections were antigen retrieved in 10 mM sodium citrate and 0.05% v/v Tween 20 (Sigma-Aldrich) at 80 °C for 30 min and then washed 3X with PBS. Primary antibodies diluted 1:100 in PBS were added overnight at 4 °C. The antibodies included, rabbit anti-Cx46[26], mouse anti-βDys (MANDAG2[7D11]; Developmental Studies Hybridoma Bank, Iowa City, IA), and rabbit anti–zonula occludens-1 (ZO-1; 40–2,200; Thermo-Fisher, Waltham, MA). After primary antibody labeling, sections were washed 4X in 0.1% v/v Tween-20 in PBS and then incubated overnight at 4 °C with fluorescently labeled secondary antibodies (1:100 in PBS) and rhodamine–wheat germ agglutinin (WGA; Vector Laboratories, Burlingame, CA; 1:100 in PBS). The sections were finally washed 4X with 0.05% v/v Tween-20 in PBS and mounted in VECTASHIELD Antifade Mounting Medium with 4',5-diamidino-2-phenylindole (DAPI; Vector Laboratories). Sections without antibody staining did not undergo antigen retrieval and were labeled with rhodamine-WGA (1:100) or fluorescein isothiocyanate (FITC)-phalloidin (1:100; Thermo-Fisher) overnight at 4 °C before washing and DAPI labeling. The 8-week-old lenses used for Cx46 labeling were fixed for 20 min at 37 °C and were not subjected to post-fixation or antigen retrieval. All the labeling was performed on three or more independent samples, with multiple images per sample collected by confocal microscopy (LSM 700; Zeiss, Jena, Germany).

Fiber morphometrics: Fiber long-side widths were measured on images from three independent samples of each genotype. We outlined a 50 µm × 50 µm square on each image, beginning about 40 µm in from the epithelial-fiber interface. Within these squares, we measured the distance between opposite vertices of each fiber cell along a line parallel to the long side of the cross-section using ZEN software (Zeiss). This resulted in 100 or more measurements per image. Statistical comparison of 3-week-old WT and Ki fiber long-side widths was performed using the Student *t* test. Statistical comparison of 8-week-old WT, Cx50 KO, and Ki fiber widths was performed using one-way analysis of variance (ANOVA). Gaussian curves were graphed based on the equation $A\alpha e^{-b}$, where A = total area of histogram, $\alpha = (2\pi\sigma^2)^{-0.5}$,

$b = (x - \mu)^2(2\sigma^2)^{-1}$, σ = standard deviation of fiber widths, and μ = mean of fiber widths.

RESULTS

Fiber cell and F-actin organization in 3-week-old lenses: In our previous study, we found regions in 3-week-old Cx50 KO lens sections with defects in fiber organization and F-actin distribution [24]. Therefore, we examined whether these phenotypes persisted in Ki lenses that also lacked Cx50. Cross-sections of WT lenses showed that fibers were radially aligned into rows, with little variation in size and shape, and F-actin staining was concentrated on and around the vertices of each fiber (Figure 1A). Ki fibers had WT-like F-actin enrichment at their vertices but displayed variations in size, with disordered alignment of rows (Figure 1B). Our quantification showed that the average fiber cell long-side width from Ki and WT lenses was similar, but Ki fibers had a much broader distribution in size (Figure 1C-D). Therefore, the misalignment appeared to be due to nonuniform fiber sizes.

Partial rescue of gap junction and ball-and-socket structures: Loss of Cx50 disrupted BS maturation and prevented the formation of large Cx46 GJ plaques, while loss of Cx46 did not noticeably affect BS or Cx50 GJ plaque assembly [24]. We examined whether BS or large GJ plaques could be restored in Ki lenses. In 3-week-old WT samples, we identified BS as regions of weakened WGA labeling, where one fiber membrane bulged into its neighboring fiber (Appendix 1). Intense and continuous Cx46 staining appeared on BS. Smaller stretches of Cx46 labeling were centered on the "flat" portions of the long sides of the hexagonal fibers. Cx46 was also dotted along the narrow sides of the fibers (Figure 2A). BSs were not seen in every field of view, but at the same time, they were not difficult to locate in any WT sample. In contrast, most regions of Ki samples showed little-to-no BSs (Appendix 1, Figure 2B). However, BSs enriched with Cx46 were occasionally observed in limited areas (Appendix 1, Figure 2C). We did not see any obvious anterior–posterior bias in the density of BSs. Outside of BSs, Ki Cx46 plaques were larger than the more punctate WT plaques (Figure 2B). We previously observed occasional regions in Cx50 KO lenses where small, balloon-like structures adjacent to the long side of fiber membranes formed [24]. They resembled small BSs that were being pinched off at their base. Such structures were rarely observed in 3-week-old Ki lenses. Thus, Ki lenses form large Cx46 GJ plaques with limited BSs.

Lack of connexin-associated protein localization to gap junctions: The multifunctional protein ZO-1 was previously shown to interact with Cx46 and Cx50, but its specific roles in the lens are unknown [25,26]. We found ZO-1 on the apical side of the epithelial layer and the vertices of peripheral fiber cells in WT samples (Figure 3A). Inner fibers (about 150–200 μm in depth) revealed a Cx-like staining pattern, including on BSs (Figure 3B). In contrast, ZO-1 in Cx50 KO lenses appeared in fiber cell nuclei and was undetectable in inner cortical fibers, suggesting an important role for Cx50 in determining ZO-1 distribution [24]. Interestingly, Ki lenses had an intermediate phenotype of ZO-1 distribution. ZO-1 was present on fiber vertices and absent in the nuclei of the most peripheral fibers, like in the WT (Figure 3C). However, like in Cx50 KO lenses, ZO-1 did not appear with a Cx-like pattern in Ki inner fibers (Figure 3D).

β-Dystroglycan (βDys) is a transmembrane glycoprotein that links the extracellular matrix (ECM) to the cytoskeleton and is important for structural integrity in various tissues [27]. Its role in lens fibers is also unknown. βDys labeled the basal membrane of lens epithelial cells and on fiber membranes with a Cx-like pattern in WT lenses (Figure 4A-B). In the Cx50 KO, βDys labeling occurred in fiber nuclei and diffusely over fiber cell membranes but showed no Cx-like staining [24]. Like ZO-1, βDys showed an intermediate phenotype in Ki lenses. It was found on the basal membrane of the epithelium, weakly over fiber cell membranes, but no longer in fiber cell nuclei nor with a Cx-like pattern on Ki fibers (Figure 4C-D).

Restored fiber cell organization in 8-week-old lenses: We next investigated whether some observed fiber cell phenotypes changed with age by imaging 8-week-old lenses. The organizations of peripheral fibers in Cx50 KO and Ki lenses were much improved when compared to those at 3 weeks. Radially stacked fiber rows were evident throughout the samples. In addition, enrichment of F-actin at the tricellular vertices of Ki and WT mice often appeared reduced when compared to their 3-week-old counterparts (Figure 5A-C). We measured WT, Cx50 KO, and Ki fiber cell long-side widths and found that they had similar size distributions and average widths, which is consistent with the improvement in fiber organization with age (Appendix 2).

Varied ball-and-socket morphologies in 8-week-old lenses: We examined 8-week-old WT, Cx50 KO, and Ki lenses to determine whether BS morphology and distribution changed with age. BS in WT lenses at 8 weeks resembled those at 3 weeks (Figure 6A). Eight-week-old Cx50 KO fibers had balloon-like structures in their cytosols like those seen in 3-week-old KO lenses (Figure 6B). Ki lenses showed diverse structures, including typical BSs, abnormally lengthened and curved BSs, and balloon-like structures (Figure 6C). BSs appeared more commonly in 8-week-old Ki lenses than

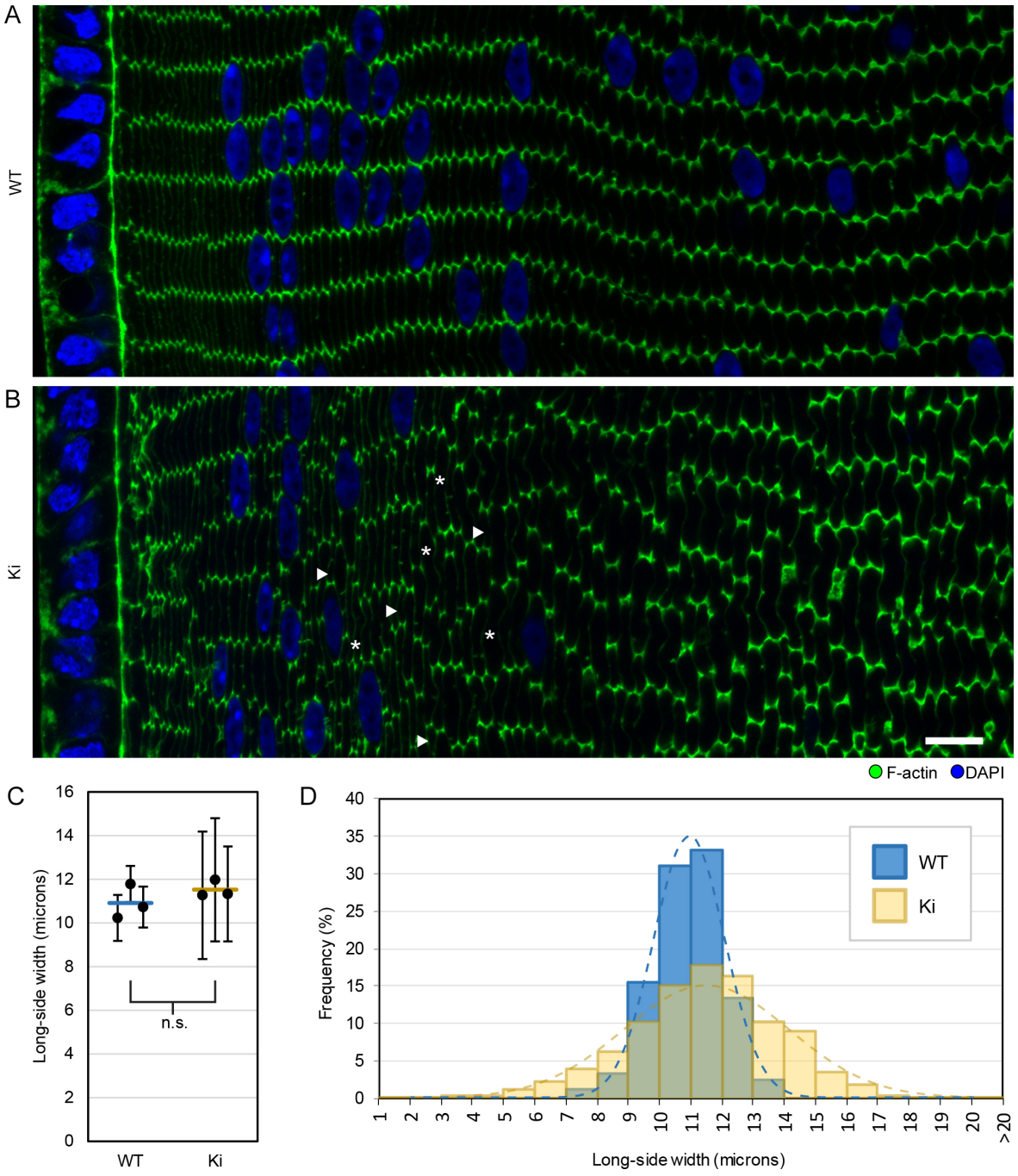

Figure 1. F-actin distribution and fiber sizes in 3-week-old wild-type (WT) and knock-in (Ki) lenses. Images of cortical fibers from equatorial sections stained with phalloidin for F-actin (green) and 4',5-diamidino-2-phenylindole (DAPI) for DNA (blue). **A:** WT hexagonal fibers are arranged in parallel rows with F-actin enriched at their vertices. **B:** Ki fibers do not have the same precise organization, but F-actin is still enriched at the vertices. Compared to WT, the widths (long axis lengths of hexagons) of Ki fibers were not uniform. Arrowheads and asterisks denote examples of short and tall fibers, respectively. Scale bar: 10 µm. **C:** Plot of the average fiber cell long-side widths from images of three WT and three Ki samples. Circles denote average fiber cell long-side width from individual samples, with error bars denoting standard deviations. Horizontal lines denote the mean of the three sample averages. The means from WT and Ki samples were not significantly different (p>0.25). **D:** Histogram compiling the distribution of fiber cell widths from the three WT and Ki samples shows that Ki fibers have a much broader distribution of widths compared to WT. Dashed lines represent Gaussian curves calculated from the mean (µ) and standard deviation (σ) of WT and Ki fibers (μ^{WT} = 10.9 µm, σ^{WT} = 1.1 µm, μ^{Ki} = 11.5 µm, σ^{Ki} = 2.6 µm).

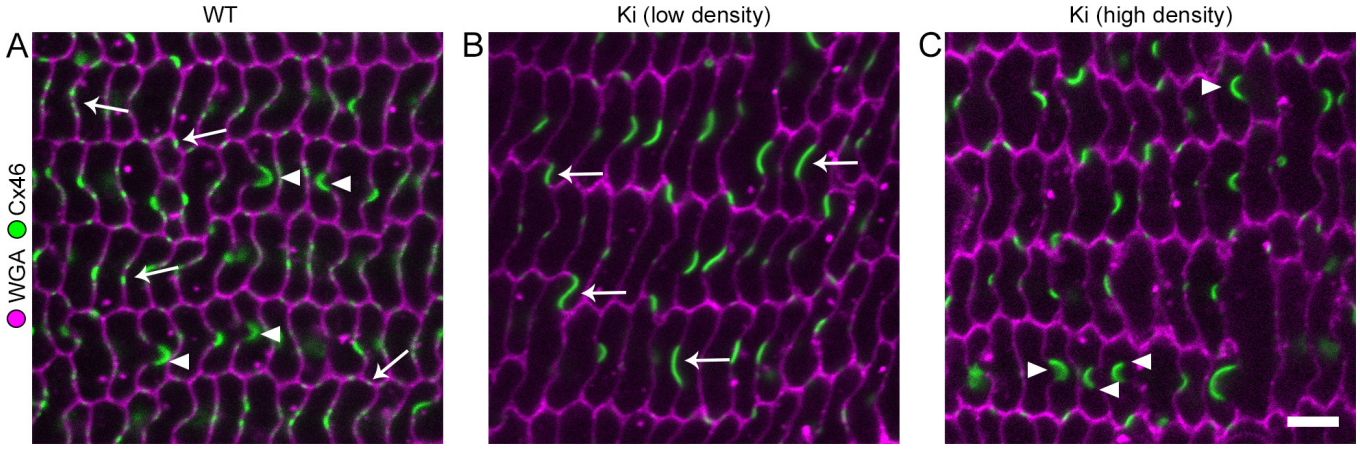

Figure 2. Retention of ball-and-sockets (BSs) at 3 weeks. **A:** Wild-type (WT) sample showing BSs (arrowheads) as connexin 46 (Cx46)-enriched areas where one fiber has invaginated into a neighboring fiber. Small Cx46 gap junction (GJ) plaques (arrows) appeared on the long and narrow sides of fibers outside of the BSs. **B:** Most regions of knock-in (Ki) fiber sections showed few to no structures resembling BSs, but many large Cx46 GJ plaques are apparent (arrows). **C:** Some limited regions still appeared to have Cx46-enriched BS structures (arrowheads). Scale bar: 5 µm.

in 3-week samples. F-actin labeling was absent or weak compared to adjacent membrane regions on both BSs and balloons (Figure 6A-C). The Cx46 staining results on 8-week-old samples show that only BSs contained enriched Cx46, while balloons had little or no Cx46 signal. Occasionally, a Cx46 signal appeared near the base of the balloons (Figure 6D-G). Ki of Cx46 seemed to partly restore BS with Cx46 GJs.

DISCUSSION

Whole-lens phenotypes, physiologic measurements, and cell-proliferation data for Ki mice have consistently shown that Ki of Cx46 can only partially rescue the defects observed in Cx50 KO lenses [21-23]. The same theme follows in the context of cortical lens fibers: Only certain fiber cell phenotypes are rescued.

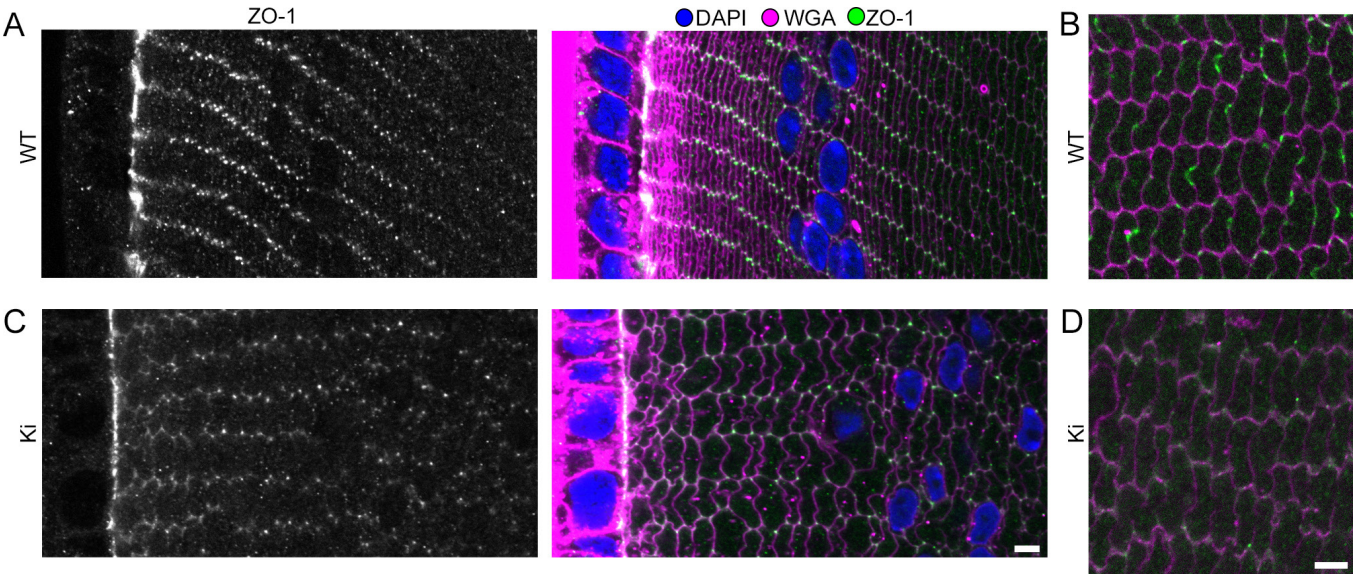

Figure 3. Zonula occludens-1 (ZO-1) distribution. **A:** In wild-type (WT) samples, ZO-1 localized to the epithelial–fiber interface and to the vertices of the most peripheral fibers. **B:** ZO-1 staining was enriched on the long and short sides of inner cortical fibers (about 150–200 µm from the surface) with a connexin (Cx)-like staining pattern. **C:** ZO-1 appeared on the epithelial–fiber interface and the vertices of knock-in (Ki) peripheral fibers. **D:** ZO-1 was not detected in inner cortical fibers of Ki lenses. Scale bars: 5 µm.

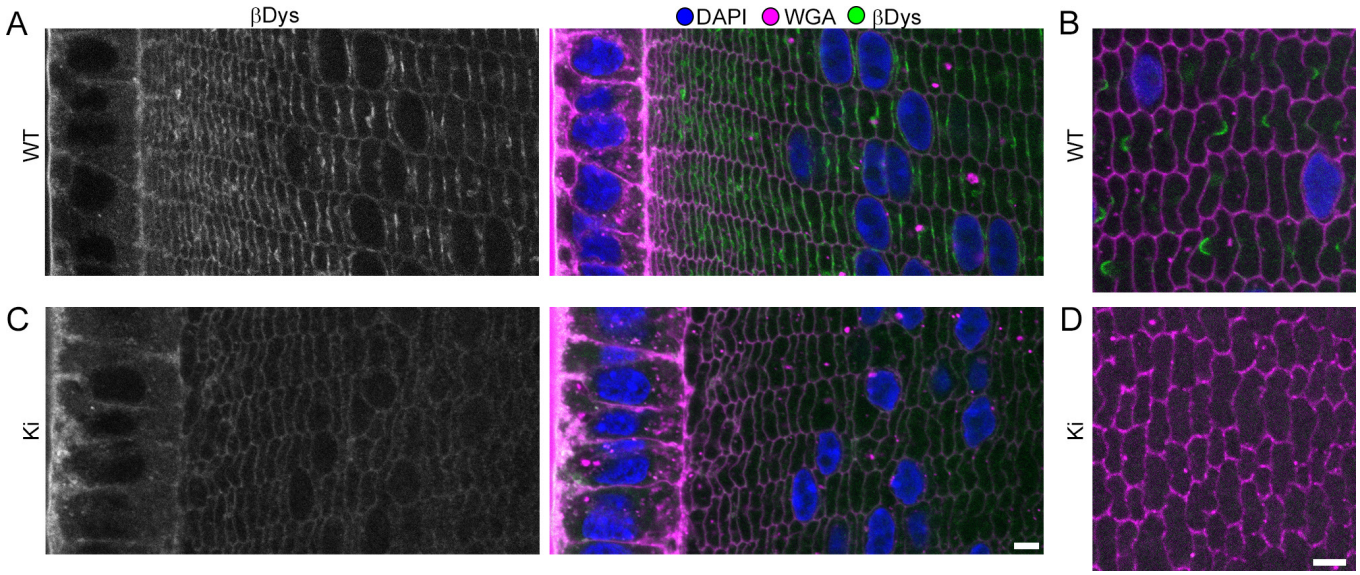

Figure 4. β-Dystroglycan (βDys) distribution. **A:** In wild-type (WT) samples, βDys localizes to the basal side of epithelial cells and on fiber membranes. The strongest βDys signals have a connexin (Cx)-like staining pattern on fiber membranes. **B:** In WT inner cortical fibers, βDys displayed Cx-like staining. **C:** In knock-in (Ki) samples, βDys is similar to WT samples in peripheral fibers, but lacks Cx-like staining. **D:** In Ki inner cortical fibers, βDys was undetectable. Scale bars: 5 µm.

We associated disorganization observed in regions of Cx50 KO lenses with reduced F-actin enrichment at fiber vertices. This premise was supported by previous connections between cytoskeletal defects and organization defects [28-31]. Even so, peripheral fibers of 3-week-old Ki lenses were also disorganized, despite showing normal F-actin distributions. Meanwhile, normal F-actin distribution and fiber organization were observed in 3-week-old *Gja3*$^{-/-}$ (Cx46 KO) lenses [24]. These observations point to Cx50 having a specific role in establishing or maintaining fiber organization. Cx50 was shown to interact with the cell-adhesive water channel, aquaporin 0 [32], so one possibility is that Cx50 GJs provide cell–cell adhesion cues that help orient fibers relative to one another. Another possibility is that Cx46 provides adhesion cues that are disrupted by the increased size and spacing of the Ki's Cx46-plaques. Finally, our results indicate that fiber organization is consistently better in 8-week-old lenses. The reduced effect on fiber phenotypes with age in Cx50-deficient lenses is consistent with previous results which showed that the weight ratios of WT to Cx50 KO lenses became constant by 8 weeks and that epithelial cell proliferation in Cx50 KO mice was mostly reduced in the early postnatal period [13,15]. Therefore, the roles of Cx50 appear to become less essential after the rapid growth phase of young lenses. The remaining Cx46 seems sufficient to support the slower growth rate of peripheral fibers in older Cx50 KO lenses.

BS structures are believed to promote rapid communication through GJs in the actively elongating and maturing cortical fibers [9]. GJs associated with BSs even have a different ultrastructure than GJs not on BSs, implying a specific function [33]. Our earlier results showed that loss of Cx50, but not loss of Cx46, led to loss of mature BSs and potentially contributed to the Cx50 KO growth defect [24]. Interestingly, the increased quantities of Cx46 in Ki lenses did result in the presence of limited BSs, meaning that BSs are not strictly Cx50-dependent structures. However, their limited occurrence in 3-week-old samples indicates that Cx46 BSs do not develop as readily as in Cx50-containing lenses. The presence of balloon-like structures in 3- and 8-week-old Cx50 lenses and 8-week-old Ki samples further indicates a handicapped ability of Cx46 to support BSs. The balloons may represent BS-like structures that did not acquire adequate GJs. Past studies showed that BSs can be initiated without Cx enrichment [9], possibly through a mechanism involving actin and clathrin [34]. If BS initiation is Cx independent, then our results point to Cx46 either having a lower affinity for BSs or having a lower ability to sustain them. We currently do not know why 8-week-old Ki lenses have increased BSs and balloons. Regardless, the observed partial rescue of BSs could contribute to the increased size of Ki lenses compared to Cx50 KO lenses.

The significant exclusion of F-actin from both balloons and BSs points to their having similar origins and may be

an important trait for their formation or growth. Spherical membrane protrusions known as blebs form during various cellular processes and occur at sites where the cortical actin network is separated from the membrane. Bleb growth is driven by intracellular pressure and cortical tension [35,36]. Similarly, the depleted cortical actin under GJs in the lens may provide regions that are more susceptible to adopting or maintaining curvature, especially if local membrane/cortical tension differs between the linked cells. This is a potential explanation for why asymmetric BSs would be sustained—especially considering GJs should be approximately symmetric and have no significant underlying actin cytoskeletal support, unlike lens fiber protrusions and neural dendrites [37,38]. (Note: BSs still form in the beaded filament deficient 129/SvJ mouse strain, suggesting that intermediate filaments are not responsible for maintaining BS asymmetry either.) Interestingly, in primates, where actin does associate with GJs after the superficial cortex, BSs do not expand to the sizes seen in mice and rabbits [8,39]. Actin exclusion is also an explanation for the lack of mature BSs in Cx50 KO lenses: Loss of large-area GJs and corresponding actin-depleted regions would mean fewer areas that would be prone to expansion of bleb-like structures. Blebs are also regions where membrane components can rapidly diffuse [40], which could promote GJ growth in the case of lens fibers. Gaps in lens fiber cortical actin–spectrin networks are associated

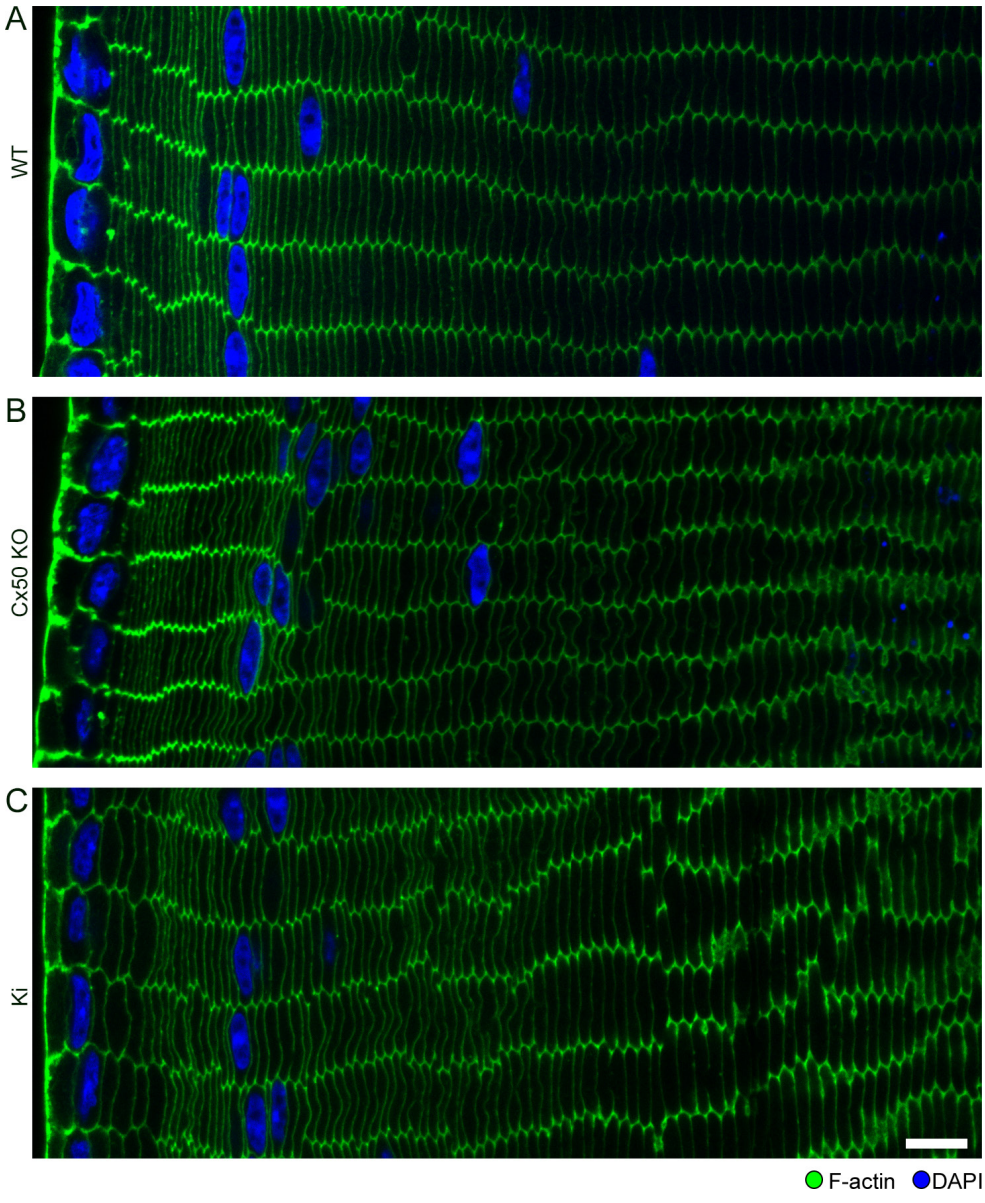

Figure 5. Fiber organization in 8-week-old lenses. **A:** Wild-type (WT) lenses retain well-organized, radially stacked rows of fiber cells in 8-week-old lenses. **B:** Disordered fiber cell regions are no longer commonly observed in connexin 50 (Cx50) knockout (KO) lenses at 8 weeks. **C:** Eight-week-old knock-in (Ki) lenses showed typical organization of overlaid fibers. Scale bar: 10 µm.

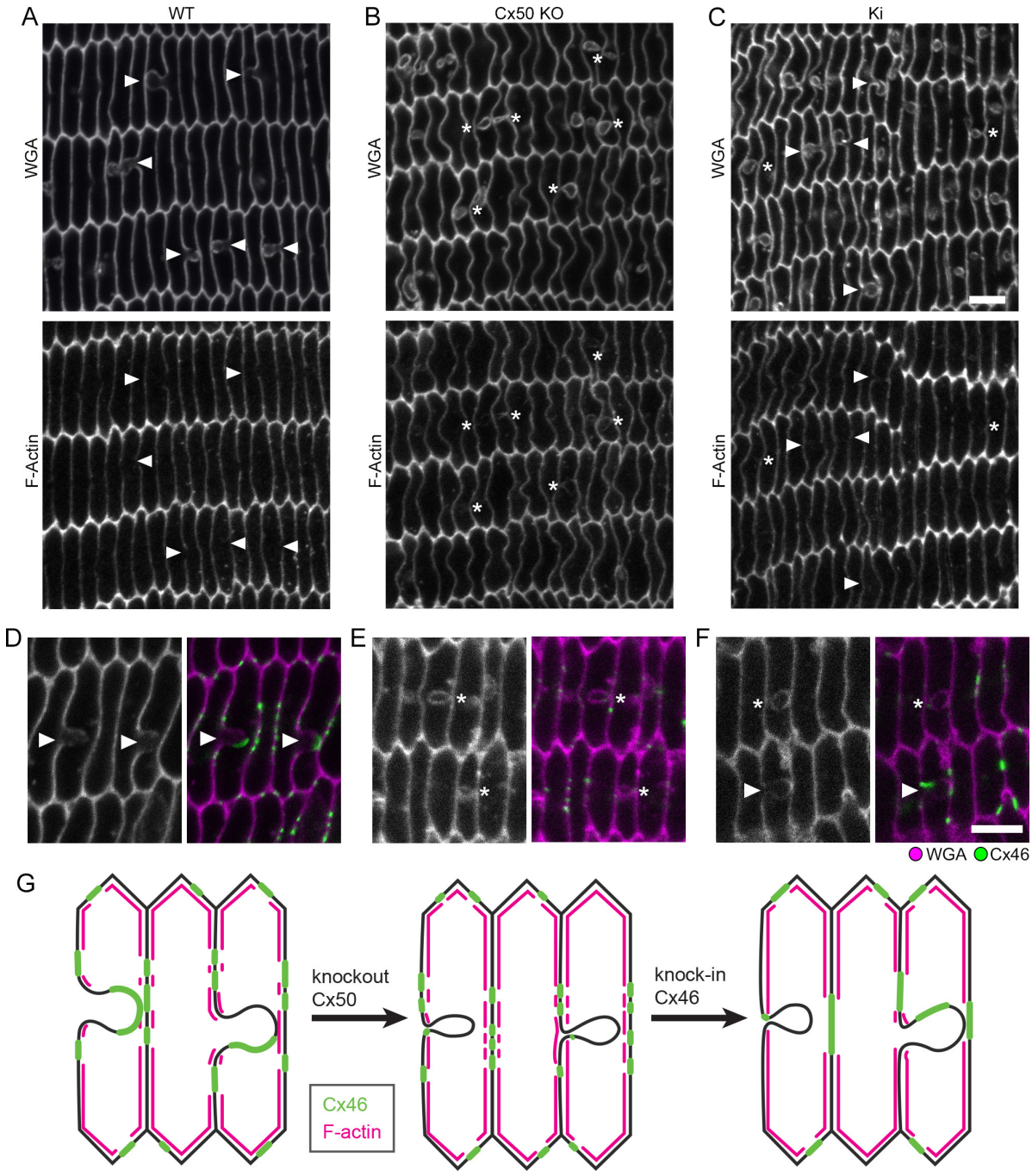

Figure 6. Ball-and-sockets (BSs) in 8-week-old lenses. **A:** BS (arrowheads) in 8-week-old wild-type (WT) lenses resemble those at 3 weeks. **B:** Connexin 50 (Cx50) knockout (KO) lenses have balloon-like structures (asterisks) that resemble BSs that are pinched at their base. **C:** Knock-in (Ki) lenses have BSs (arrowheads) and balloon-like structures (asterisks). **D**-**F:** Cx46 is enriched on BSs (arrowheads) but absent or nearly absent from balloon-like structures (asterisks). Images taken approximately 100 µm from the sample edge. Scale bar: 5 µm. **G:** Schematic of Cx46 (green) and F-actin (magenta) distributions relative to BSs and balloons in 8-week-old WT, Cx50 KO, and Ki lenses.

with GJs [41], suggesting that GJs mediate F-actin exclusion. However, the lack of significant quantities of GJs in the actin-depleted balloons implies that a GJ-independent process may also occur.

Interactions between Cx and the postsynaptic density 95/*Drosophila* disk large/ZO-1 (PDZ)-domain containing protein ZO-1 are varied and cell-type dependent. ZO-1 has roles in GJ assembly, disassembly, and remodeling that depend on cell type, Cx isoform, and posttranslational Cx modifications [25,42-44]. Our results in Ki and Cx50 KO mice all indicate that Cx50 is required for enrichment of ZO-1 to GJs on inner cortical fibers. The depth at which ZO-1 enrichment occurs coincides with significant modifications to Cx46 and Cx50, including truncation of their C-terminals, which contain their PDZ-binding motifs [45,46]. Therefore, ZO-1 may act to initiate these remodeling events [25]. Interestingly, truncation of Cx46 C-termini is significantly delayed in Ki lenses, so even with a PDZ-binding motif that remains intact, Cx46 did not promote ZO-1 colocalization [47]. Our results also indicate that ZO-1 may be unessential to BSs. Interactions between Cx46 and ZO-1 were previously shown by coimmunoprecipitation [25]. We suspect that the nature or amount of Cx46–ZO-1 interactions is such that we are unable to clearly detect them by immunofluorescent imaging.

Both the Cx50 KO and Ki results indicate that βDys enrichment at GJs also requires the Cx50 isoform. However, βDys's role in fiber cells and relation to Cx are unknown. Dystroglycan is associated with complexes that link the actin cytoskeleton to the ECM [48] and is important for the clustering of certain transmembrane proteins [49,50]. However, neither actin nor ECM components are associated with fiber GJs, and Dystrophin (Dp71), a common partner for βDys, does not show a similar GJ-enriched staining pattern in the lens [51]. Therefore, fiber GJ-associated βDys may have an atypical function. No Cx isoforms have been reported to directly interact with βDys. Double KO of Cx30 and Cx43 reduces hippocampal levels of βDys, but this occurs through an unelaborated pathway [52]. Decreased βDys was observed in aged Ankyrin-B+/− mice, although the mechanism of this disruption and its effects on Cx, if any, require further study [53]. Therefore, the mechanism associating βDys with Cx50-associated GJs remains to be determined.

Importantly, the products of Cx46 alleles expressed from Cx50 loci ($Cx46_{50}$) may not be equivalent to Cx46 expressed from its native loci ($Cx46_{46}$). Previous work showed that conductance through peripheral fibers is pH insensitive in Cx50 KO mice, implying that $Cx46_{46}$ is pH insensitive in the absence of Cx50 [54]. However, Martinez-Wittingham et al. showed that conductance in WT and Ki peripheral fibers is pH sensitive, suggesting that $Cx46_{50}$ is pH sensitive and can induce pH gating of $Cx46_{46}$. They posited that these inconsistent pH behaviors could be the result of different post-translational processing steps acting on $Cx46_{50}$ and $Cx46_{46}$ [23]. Therefore, we need to keep in mind that there may be separate pools of Cx46 that could be responsible for some of the phenotypes we observed.

In summary, our results provide further insight into the distinct and redundant functions of Cx50 and Cx46 in peripheral lens fibers. Cx46 supplementation can only partially restore WT-like lens fiber phenotypes to mice lacking Cx50. Fiber organization and BS maturation defects remain, especially in young (3-week-old) mice. Discovering the biomolecules that are essential to BS formation or maturation will be critical to further understanding whether they serve a unique function.

APPENDIX 1. IDENTIFICATION OF BS WITH WGA-LABELING.

To access the data, click or select the words "Appendix 1." (A) BS are identifiable in WT samples as regions of weakened WGA staining where one fiber appears to bulge into its neighbor. (B) Most regions of 3-wk-old Ki samples had very few obvious BS. (C) Limited regions of 3-wk-old Ki samples had higher densities of BS-like structures. Arrowheads denote BS. Scale bar: 5 µm.

APPENDIX 2. 8-WK-OLD FIBER CELL LONG-SIDE WIDTHS.

To access the data, click or select the words "Appendix 2." The mean fiber cell long-side widths (circles) for each of three samples from WT, Cx50 KO, and Ki lenses. Error bars denote standard deviations. Horizontal lines denote the average of the three sample averages for each genotype. One-way ANOVA suggests no significant differences in average fiber width between the three genotypes ($p>0.6$).

ACKNOWLEDGMENTS

Supported by National Institutes of Health Grant RO1EY013849 (XG).

REFERENCES

1. Söhl G, Willecke K. Gap junctions and the connexin protein family. Cardiovasc Res 2004; 62:228-32. [PMID: 15094343].
2. Mathias RT, White TW, Gong X. Lens Gap Junctions in Growth, Differentiation, and Homeostasis. Physiol Rev 2010; 90:179-206. [PMID: 20086076].

3. Koval M, Molina SA, Burt JM. Mix and match: Investigating heteromeric and heterotypic gap junction channels in model systems and native tissues. FEBS Lett 2014; 588:1193-204. [PMID: 24561196].
4. Jiang JX. Gap Junctions or Hemichannel-Dependent and Independent Roles of Connexins in Cataractogenesis and Lens Development. Curr Mol Med 2010; 10:851-63. [PMID: 21091421].
5. Wei CJ, Xu X, Lo CW. Connexins and cell signaling in development and disease. Annu Rev Cell Dev Biol 2004; 20:811-38. [PMID: 15473861].
6. Zhou JZ, Jiang JX. Gap junction and hemichannel-independent actions of connexins on cell and tissue functions – An update. FEBS Lett 2014; 588:1186-92. [PMID: 24434539].
7. Verheule S, Kaese S. Connexin diversity in the heart: insights from transgenic mouse models. Front Pharmacol 2013; 4:14-[PMID: 23818881].
8. Harding CV, Susan S, Murphy H. Scanning Electron Microscopy of the Adult Rabbit Lens. Ophthalmic Res 1976; 8:443-55. .
9. Biswas SK, Lee JE, Brako L, Jiang JX, Lo WK. Gap junctions are selectively associated with interlocking ball-and-sockets but not protrusions in the lens. Mol Vis 2010; 16:2328-41. [PMID: 21139982].
10. Kuszak JR, Zoltoski RK, Sivertson C. Fibre cell organization in crystalline lenses. Exp Eye Res 2004; 78:673-87. [PMID: 15106947].
11. Bassnett S, Shi Y, Vrensen GF. Biological glass: structural determinants of eye lens transparency. Philos Trans R Soc Lond B Biol Sci 2011; 366:1250-64. [PMID: 21402584].
12. Gong X, Li E, Klier G, Huang Q, Wu Y, Lei H, Kumar NM, Horwitz J, Gilula NB. Disruption of α3 Connexin Gene Leads to Proteolysis and Cataractogenesis in Mice. Cell 1997; 91:833-43. [PMID: 9413992].
13. White TW, Goodenough DA, Paul DL. Targeted Ablation of Connexin50 in Mice Results in Microphthalmia and Zonular Pulverulent Cataracts. J Cell Biol 1998; 143:815-25. [PMID: 9813099].
14. Rong P, Wang X, Niesman I, Wu Y, Benedetti LE, Dunia I, Levy E, Gong X. Disruption of Gja8 (α8 connexin) in mice leads to microphthalmia associated with retardation of lens growth and lens fiber maturation. Development 2002; 129:167-74. [PMID: 11782410].
15. Sellitto C, Li L, White TW. Connexin50 Is Essential for Normal Postnatal Lens Cell Proliferation. Invest Ophthalmol Vis Sci 2004; 45:3196-202. [PMID: 15326140].
16. Shakespeare TI, Sellitto C, Li L, Rubinos C, Gong X, Srinivas M, White TW. Interaction between Connexin50 and Mitogen-activated Protein Kinase Signaling in Lens Homeostasis. Mol Biol Cell 2009; 20:2582-92. [PMID: 19321662].
17. Martinez JM, Wang H-Z, Lin RZ, Brink PR, White TW. Differential regulation of Connexin50 and Connexin46 by PI3K signaling. FEBS Lett 2015; 589:1340-5. [PMID: 25935417].
18. Banks EA, Yu XS, Shi Q, Jiang JX. Promotion of lens epithelial-fiber differentiation by the C-terminus of connexin 45.6 - a role independent of gap junction communication. J Cell Sci 2007; 120:3602-12. [PMID: 17895360].
19. Shi Q, Gu S, Yu XS, White Thomas W, Banks Eric A, Jiang Jean X. Connexin Controls Cell-Cycle Exit and Cell Differentiation by Directly Promoting Cytosolic Localization and Degradation of E3 Ligase Skp2. Dev Cell 2015; 35:483-96. [PMID: 26585299].
20. Slavi N, Rubinos C, Li L, Sellitto C, White TW, Mathias R, Srinivas M. Cx46 Gap Junctions Provide a Pathway for the Delivery of Glutathione to the Lens Nucleus. J Biol Chem 2014; [PMID: 25294879].
21. White TW. Unique and redundant connexin contributions to lens development. Science 2002; 295:319-20. [PMID: 11786642].
22. White TW, Gao Y, Li L, Sellitto C, Srinivas M. Optimal Lens Epithelial Cell Proliferation Is Dependent on the Connexin Isoform Providing Gap Junctional Coupling. Invest Ophthalmol Vis Sci 2007; 48:5630-7. [PMID: 18055813].
23. Martinez-Wittinghan FJ, Sellitto C, White TW, Mathias RT, Paul D, Goodenough DA. Lens gap junctional coupling is modulated by connexin identity and the locus of gene expression. Invest Ophthalmol Vis Sci 2004; 45:3629-37. [PMID: 15452070].
24. Wang E, Geng A, Maniar AM, Mui BWH, Gong X. Connexin 50 Regulates Surface Ball-and-Socket Structures and Fiber Cell OrganizationCx50 in BS Structures and Fiber Cell Organization. Invest Ophthalmol Vis Sci 2016; 57:3039-46. [PMID: 27281269].
25. Chai ZF, Goodenough DA, Paul DL. Cx50 requires an intact PDZ-binding motif and ZO-1 for the formation of functional intercellular channels. Mol Biol Cell 2011; 22:4503-12. [PMID: 21965293].
26. Nielsen PA, Baruch A, Shestopalov VI, Giepmans BNG, Dunia I, Benedetti EL, Kumar NM. Lens Connexins α3Cx46 and α8Cx50 Interact with Zonula Occludens Protein-1 (ZO-1). Mol Biol Cell 2003; 14:2470-81. [PMID: 12808044].
27. Sgambato A, Brancaccio A. The dystroglycan complex: From biology to cancer. J Cell Physiol 2005; •••:205-[PMID: 15920757].
28. Nowak RB, Fowler VM. Tropomodulin 1 Constrains Fiber Cell Geometry during Elongation and Maturation in the Lens Cortex. J Histochem Cytochem 2012; 60:414-27. [PMID: 22473940].
29. Maddala R, Deng P-F, Costello JM, Wawrousek EF, Zigler JS, Rao VP. Impaired cytoskeletal organization and membrane integrity in lens fibers of a Rho GTPase functional knockout transgenic mouse. Lab Invest 2004; 84:679-92. [PMID: 15094715].
30. Maddala R, Reneker LW, Pendurthi B, Rao PV. Rho GDP Dissociation Inhibitor-Mediated Disruption of Rho GTPase Activity Impairs Lens Fiber Cell Migration, Elongation and Survival. Dev Biol 2008; 315:217-31. [PMID: 18234179].

31. Rao PV. The pulling, pushing and fusing of lens fibers: A role for Rho GTPases. Cell Adhes Migr 2008; 2:170-3. [PMID: 19262112].

32. Liu J, Xu J, Gu S, Nicholson BJ, Jiang JX. Aquaporin 0 enhances gap junction coupling via its cell adhesion function and interaction with connexin 50. J Cell Sci 2011; 124:198-206. [PMID: 21172802].

33. Lo WK, Reese TS. Multiple structural types of gap junctions in mouse lens. J Cell Sci 1993; 106:227-35. [PMID: 8270626].

34. Zhou C-J, Lo W-K. Association of clathrin, AP-2 adaptor and actin cytoskeleton with developing interlocking membrane domains of lens fibre cells. Exp Eye Res 2003; 77:423-32. [PMID: 12957142].

35. Tinevez J-Y, Schulze U, Salbreux G, Roensch J, Joanny J-F, Paluch E. Role of cortical tension in bleb growth. Proc Natl Acad Sci USA 2009; 106:18581-6. [PMID: 19846787].

36. Charras GT, Coughlin M, Mitchison TJ, Mahadevan L. Life and times of a cellular bleb. Biophys J 2008; 94:1836-53. [PMID: 17921219].

37. Cheng C, Nowak RB, Biswas SK, Lo W-K, FitzGerald PG, Fowler VM. Tropomodulin 1 Regulation of Actin Is Required for the Formation of Large Paddle Protrusions Between Mature Lens Fiber CellsTmod1 and Lens Fiber Cell Interdigitations. Invest Ophthalmol Vis Sci 2016; 57:4084-99. [PMID: 27537257].

38. Lin Y-C, Koleske AJ. Mechanisms of Synapse and Dendrite Maintenance and Their Disruption in Psychiatric and Neurodegenerative Disorders. Annu Rev Neurosci 2010; 33:349-78. [PMID: 20367247].

39. Lo W-K, Mills A, Kuck JFR. Actin Filament Bundles are Associated with Fiber Gap Junctions in the Primate Lens. Exp Eye Res 1994; 58:189-96. [PMID: 8157111].

40. Saha S, Lee I-H, Polley A, Groves JT, Rao M, Mayor S. Diffusion of GPI-anchored proteins is influenced by the activity of dynamic cortical actin. Mol Biol Cell 2015; 26:4033-45. [PMID: 26378258].

41. Cheng C, Nowak RB, Gao J, Sun X, Biswas SK, Lo W-K, Mathias RT, Fowler VM. Lens ion homeostasis relies on the assembly and/or stability of large connexin 46 gap junction plaques on the broad sides of differentiating fiber cells. Am J Physiol Cell Physiol 2015; 308:C835-47. [PMID: 25740157].

42. Barker RJ, Price RL, Gourdie RG. Increased Co-localization of Connexin43 and ZO-1 in Dissociated Adult Myocytes. Cell Commun Adhes 2001; 8:205-8. [PMID: 12064589].

43. Laing JG, Chou BC, Steinberg TH. ZO-1 alters the plasma membrane localization and function of Cx43 in osteoblastic cells. J Cell Sci 2005; 118:2167-76. [PMID: 15855237].

44. Dunn CA, Lampe PD. Injury-triggered Akt phosphorylation of Cx43: a ZO-1-driven molecular switch that regulates gap junction size. J Cell Sci 2014; 127:455-64. [PMID: 24213533].

45. Lin JS, Fitzgerald S, Dong Y, Knight C, Donaldson P, Kistler J. Processing of the gap junction protein connexin50 in the ocular lens is accomplished by calpain. Eur J Cell Biol 1997; 73:141-9. [PMID: 9208227].

46. Jacobs MD, Soeller C, Sisley AMG, Cannell MB, Donaldson PJ. Gap Junction Processing and Redistribution Revealed by Quantitative Optical Measurements of Connexin46 Epitopes in the Lens. Invest Ophthalmol Vis Sci 2004; 45:191-9. [PMID: 14691173].

47. Gao J, Sun X, Martinez-Wittinghan FJ, Gong X, White TW, Mathias RT. Connections Between Connexins, Calcium, and Cataracts in the Lens. J Gen Physiol 2004; 124:289-300. [PMID: 15452195].

48. Moore CJ, Winder SJ. Dystroglycan versatility in cell adhesion: a tale of multiple motifs. Cell Commun Signal 2010; 8:1-12. [PMID: 20163697].

49. Jacobson C, Côté PD, Rossi SG, Rotundo RL, Carbonetto S. The Dystroglycan Complex Is Necessary for Stabilization of Acetylcholine Receptor Clusters at Neuromuscular Junctions and Formation of the Synaptic Basement Membrane. J Cell Biol 2001; 152:435-50. [PMID: 11157973].

50. Noell S, Wolburg-Buchholz K, Mack AF, Beedle AM, Satz JS, Campbell KP, Wolburg H, Fallier-Becker P. Evidence for a role of dystroglycan regulating the membrane architecture of astroglial endfeet. Eur J Neurosci 2011; 33:2179-86. [PMID: 21501259].

51. Fort PE, Darche M, Sahel J-A, Rendon A, Tadayoni R. Lack of dystrophin protein Dp71 results in progressive cataract formation due to loss of fiber cell organization. Mol Vis 2014; 20:1480-90. [PMID: 25489223].

52. Ezan P, André P, Cisternino S, Saubaméa B, Boulay A-C, Doutremer S, Thomas M-A, Quenech'du N, Giaume C, Cohen-Salmon M. Deletion of astroglial connexins weakens the blood–brain barrier. J Cereb Blood Flow Metab 2012; 32:1457-67. [PMID: 22472609].

53. Maddala R, Walters M, Brophy PJ, Bennett V, Rao PV. Ankyrin-B directs membrane tethering of periaxin and is required for maintenance of lens fiber cell hexagonal shape and mechanics. Am J Physiol Cell Physiol 2016; 310:C115-26. [PMID: 26538089].

54. Baldo GJ, Gong X, Martinez-Wittinghan FJ, Kumar NM, Gilula NB, Mathias RT. Gap Junctional Coupling in Lenses from α8 Connexin Knockout Mice. J Gen Physiol 2001; 118:447-56. [PMID: 11696604].

Articles are provided courtesy of Emory University and the Zhongshan Ophthalmic Center, Sun Yat-sen University, P.R. China. The print version of this article was created on 24 March 2017. This reflects all typographical corrections and errata to the article through that date. Details of any changes may be found in the online version of the article.